Received: 21 May 2023 | Revised: 24 June 2023 | Accepted: 24 June 2023

DOI: 10.1111/azo.12477

ORIGINAL ARTICLE

Acta Zoologica | WILEY

SnoRNAs may accelerate protein synthesis for the rapid growth of the regenerating tail blastema in the lizard *Podarcis muralis*

Massimo Degan[1,2] | **Lorenzo Alibardi**[1,2]

[1]Centro di Riferimento Oncologico (CRO), Aviano, Italy

[2]Comparative Histolab Padova, Padova, Italy

Correspondence
Lorenzo Alibardi, Dipartimento di Biologia, Universita di Bologna, Via Selmi 3, 40126 Bologna, Italy.
Email: lorenzo.alibardi@unibo.it

Funding information
Centro di Riferimento Oncologico, Aviano, PN and Comparative Histolab Padova

Abstract

Tail regeneration in lizards derives from the formation of a regenerative blastema. Numerous snoRNAs exclusively up-regulated in the regenerating tail but absent in the scarring limb of the lizard *Podarcis muralis* have been detected suggesting they are key genes for regeneration. While most snord-, snora- and scarna-RNAs are activators of protein synthesis and cell proliferation (oncogenes) some may also be tumour suppressors. A tail blastema of 2–3 mm in length consists of proliferating mesenchymal cells, fibroblasts and keratinocytes with active nucleoli, rosette-patterned ribosomes and few rough endoplasmic cisternae. In few days, the blastema grows into a new tail indicating intense protein synthesis within this short period. A quantitative RT-PCR analysis of *snord87*, *snord26*, *snord74*, *snora63*, *scarna11*, *U2* and *U4* shows that, aside *snord87*, the other ncRNAs are up-regulated, particularly, *U2*, *U4* and *scarna11*. These ncRNAs might regulate the rate of production of ribosomes from the nucleolus (snora- and snord-RNAs), the splicing process (snord- and scarna-RNAs, U2 and U4), the speed of protein synthesis (snora- and snord-RNAs) and cell proliferation in the blastema. These non-coding-RNAs are hypothesized to intensify the production of more functional ribosomes that accelerate the rate of protein synthesis and rapid growth of the blastema into a new tail.

KEYWORDS

lizard, regenerating tail, ribosomes, RT-PCR, snoRNAs, ultrastructure

1 | INTRODUCTION

Anamniotes (fish and amphibians) show regenerative capabilities that are absent in amniotes, the terrestrial-adapted vertebrates that include ectothermic reptiles and endothermic birds and mammals (Alibardi, 2022; Grygorian, 2021; Mescher, 2017; Reichman, 1984). However, as a peculiar case among amniotes, lizards can regenerate a large and histologically complex organ, the tail (Alibardi, 2014; Alibardi & Sala, 1983, 1988; Cox, 1969; Fisher et al., 2012; Gilbert et al., 2015; Lozito & Tuan, 2016). Lizards can also repair long bones, vertebrae and knees after extensive damages (Alibardi, 2015, 2021; Pritchard & Ruzicka, 1951). These reptiles appear to possess higher healing capabilities than other amniotes that may be in relation with the evolution of autotomy, the voluntary mechanism of self-amputation of the tail. In contrast, after the amputation of their digits or limbs the ability of regeneration is quite limited since these appendages usually form short scars and only occasionally short tail-like outgrowths of few millimetres (Alibardi, 2016, 2021; Bellairs & Bryant, 1968).

In order to discover genes responsible for the stimulation of organ regeneration in lizards, as a regenerative model for all amniotes, recent molecular studies have indicated that the tail but not the limb assumes embryonic characteristics in relation to gene expression after amputation (Degan et al., 2020; Hutchins et al., 2014; Patel et al., 2022; Vitulo et al., 2017a, 2017b). The capability to regenerate the tail but not the limb is a unique case among vertebrates, indicating that the same animal can evocate a broad regenerative process in a region of the body, the tail and a contemporaneous scarring process in a nearby region, the limb. The activation of genes for a different development programme in the tail versus the limb is challenging. This idea has been developed in designing a transcriptome study that has produced important information on the regenerative programme activated in the tail in comparison with that activated in the limb of the same animal (Vitulo et al., 2017a, 2017b). In fact, the comparison between genes that are up-regulated and down-regulated in the tail versus those of the limb in the same lizard has allowed the identification of some key genes that determine regeneration in lizards and, possibly, also in other amniotes. Both coding and non-coding genes, mainly in the Wnt signalling pathways and snoRNAs (small nucleolar RNAs) that are exclusively up-regulated in the regenerating tail blastema have been identified, but they are absent in the injured limb destined to scar. The non-coding RNAs (ncRNAs) include snoRNAs, micro-RNAs (miRNAs) and other ncRNAs (Dupuis-Sandoval et al., 2015; Makarova et al., 2013; McMahon et al., 2015). The ncRNAs are important for the regulation of gene activity in different cells, particularly during embryonic processes and some exclusive ncRNAs are present only in the regenerating tail but not in the healing limb. Therefore, ncRNAs represent important gene products to study in addition to the key coding genes of tail regeneration previously detected in the lizard *Podarcis muralis* (Vitulo et al., 2017a, 2017b).

The regenerating blastema of *Podarcis sicula* and *P. muralis* is formed by a loose connective tissue mainly containing proliferating fibroblasts (fusiform) and mesenchymal cells (more irregular-shaped; see Alibardi, 2010, 2016, 2019b; Alibardi & Sala, 1988). The blastema has a different histological composition from that of the normal tail where numerous differentiated tissues are present but almost no mesenchymal cells. During the regeneration of lizard tail, various micro-RNAs (miRNAs; Hutchins et al., 2016) and snoRNAs (Alibardi, 2019a, 2022; Vitulo et al., 2017a) are up-regulated. Exclusive ncRNAs that are up-regulated (27–41-folds in the transcriptome) in the blastema cone of the tail in *Podarcis muralis* but not in the scarring limb, include snoRNAs such as *snora63*, *snord74*, *scarna11* and *snord26*. Based on the few functional information, it has been hypothesized that the first three genes act as oncogenes while the last one may function as a tumour suppressor, but the specific role of these ncRNAs in the blastema remains to be further analysed.

In order to progress in the understanding of the role of exclusive genes in the regenerating lizard tail, we have re-analysed the expression of some ncRNAs using quantitative PCR. Coupling these data with an electron microscopy analysis of blastema cells we suggest that the increase in protein synthesis in the blastema of *P. muralis* derives from the formation of more efficient ribosomes for protein synthesis in blastema cells in comparison with the ribosomes of the cells forming the normal tail.

2 | MATERIALS AND METHODS

2.1 | Bioinformatics analysis of the sequences in *Podarcis muralis*

The present, theoretical and bioinformatic study, has utilized the database generated during the transcriptome sequencing of the regenerating tail and limb blastemas from the wall lizard (*Podarcis muralis*; Vitulo et al., 2017a). The following non-coding genes were analysed for expression using quantitative PCR (Q-PCR, see below): *snord87*, *snord26*, *snord74*, *snora63*, *scarna11*, *U2* and *U4* (Figure S1).

2.2 | Animals and tissue collections

After inducing autotomy in four adult lizards (*Podarcis muralis*), a natural process of tail auto-amputation, the tail was released and the lizards were kept in cages for about 1 month, and they were fed with mealworms and maggots. The study was conducted following the Italian regulations for handling vertebrates under experiment (Art. 5, DL 116/92). The proximal part of about 3 mm of the lost tail in four lizards served for collecting the control tissues that were immediately utilized for RNA extraction. On this purpose, the tail was rapidly fragmented into tiny pieces in TRIZOL (Invitrogen) at 0–4°C, left for 3–4 h at 4°C, and then stored for few days at −25°C, and later stored at −80°C until use. This initial material was considered as the Normal Tail Control (NTC) for the following regenerated tails that were derived from the same lizards. On that purpose, after the tails of the lizards formed regenerating cones of about 3 mm in length in about 14–16 days at 26–30°C, we collected the regenerating tissues in hypothermic conditions (leaving the animals for about 10 min at 4°C), by cutting the tissues with a razor blade. The latter samples were indicated as regenerating tail (RegT).

2.3 | Histology and transmission electron microscopy

The tail from three adult lizards (*Podarcis muralis*) was collected in previous studies (Alibardi, 2016, 2017, 2019b), and some new histological sections were obtained for the present report. The blastemas were fixed in 2.5% glutaraldehyde in phosphate buffer (0.2 M at pH 7.2), rinsed in buffer and osmicated for 1 h in 2% OsO_4, rinsed again in buffer and in distilled water, dehydrated in ethanol, and embedded in Durcupan Resin. Using an ultramicrotome, tissues embedded in Durcupan were sectioned at 1–2 μm thickness, and the collected sections were deposited on glass slides and left to dry. Some of these sections were stained with 1% toluidine blue for histological examination and photography. From selected areas of the samples, thin sections in Durcupan (40–50 mn thick) were collected on copper grids, stained with uranyl acetate and lead citrate according to routine methods, dried and observed under a Zeiss 10C/CR electron microscope operating at 60 kV.

Other three lizards were injected with 5BrdU to study cell proliferation, as previously reported (Alibardi, 2016), and the tissues were included in the Resin Bioacryl (Scala et al., 1992). Tissues were sectioned for the immunohistochemical localization of 5BrdU in cells that indicate their DNA is replicating and indicating cell proliferation. On this purpose the blastemas were fixed in a 4% solution of paraformaldehyde in phosphate buffer, rinsed in buffer, dehydrated in ethanol and embedded in Bioacryl resin. For light microscopy immunocytochemistry, the sections were incubated overnight at 0–4°C with a mouse antibody against 5BrdU (purchased from DBHB, University of Iowa, USA) at concentration of 1:100 diluted in Buffer Tris 0.05 M at pH 7.6 containing 1% BSA. In controls, no antibody was used. The sections were rinsed in buffer and incubated for 60 min at room temperature with a rhodamine-conjugated anti-mouse antibody (TRITC, Sigma, diluted 1:100), rinsed in the buffer, mounted in Fluoroshield anti-fading medium (Sigma) and observed under a fluorescence microscope equipped with a fluorescein filter and a digital camera.

Selected 60–90 nm thick sections, collected on nickel grids were used for the immunogold electron microscopic examination. The sections were incubated for 3 h at room temperature in the primary antibody diluted in 0.05 M TRIS–HCl buffer at pH 7.6, containing 1% cold water fish gelatin. In controls, the primary antibody was omitted. The sections were rinsed in buffer and incubated for 1 h at room temperature with anti-mouse gold-conjugated secondary antibodies (Sigma, 10 nm gold particles). Some sections went through the silver enhancement technique for increasing the size of gold particles using the kit and protocol indicated by the manufacturer (British Biocell, cat. SEKB250). After the immunoreaction, the grids were rinsed in buffer, dried and stained for 4 min with 2% uranyl acetate, and then observed and photographed under an electron microscope Zeiss 10C/CR using a digital camera.

2.4 | RNA extraction and DNA preparation

Total RNA from normal tails (NTC) and regenerating tail (RegT) tissues from three lizards were separately extracted using TRIzol Reagent (Invitrogen, Thermo Fisher Scientific) according to the manufacturer's instructions. After pooling the extracted RNA from three adult lizards into a single vial for each tissue type (NTC and RegT), 1 μg of pooled RNA from each tissue, after treatment with DNAse, was reverse transcribed into first strand cDNA by ImProm-II System reverse transcription (Promega Co.) in a 20 μL reaction mix containing hexadeoxyribonucleotide random primers (0.5 μg) for 1.0 h at 42°C.

2.5 | Primer selection and RT-PCR

Before to proceeding with the setting up of the Q-PCR experiments, primers were selected on conserved regions between the specific reference sequence of transcriptome fragments available for *P. muralis* (National Center for Biotechnology Information, NCBI, Gene Bank analysis) and *Anolis Carolensis* (Ensamble gene annotation browser). The identity range obtained by comparing the aligned *Podarcis* and *Anolis* reference sequences ranged from a minimum of 78% (Scarna11) up to 100% (U4 spliceosomal RNA). Each primer pair was selected by comparing the gene regions with the greatest similarity between the aligned sequences of *Podarcis* and *Anolis*. Primers sequences for the 7 ncRNAs are reported in Figure S1. The expression of 7 ncRNAs selected genes in NTC and RegT was analysed by RQ-PCR performed with CFX96 Real-Time PCR Detection System (BIO-RAD), using 1 μL of cDNA sample, 10 pmol of forward and reverse specific gene primers and 5 μL of 2× SYBR Select Master Mix (Applied Biosystems) in 10 μL of total final volume, following the manufacturer's instructions. Quantitation of NTC and RegT were also normalized and analysed for the expression of *Podarcis muralis* glyceraldehyde-3-phosphate dehydrogenase (gapdh) housekeeping gene to account in the initial concentration and quality of the total RNA. The analyses were performed in triplicate and a negative control (no template RNA) was included within each experiment. SYBR select RQ-PCR was performed

initially for 4′ at 94°C, followed by 44 cycles of 20″ at 94°C, 30″ at 60°C and 30″ at 72°C, followed by 1′ at 95°C, 1′ at 70°C, 7″ at 70°C with a temperature increase every 0.3″ up to 95.5°C. The relative expression in each gene studied was calculated utilizing the expression level of *gapdh* (glycerophosphate-3-dehydrogenase) gene as internal control using the equation $2^{-\Delta C_t}$, where $\Delta C_t = \left(C_{t_{gene}} - C_{t_{gapdh}}\right)$. Changes in folds of expression between classes were calculated as previously reported (Bomben et al., 2010). The data were expressed as fold change induction ± SD and the results were compared with Student's *t*-test analysis.

3 | RESULTS

3.1 | Main cell types and cell proliferation in the regenerating blastema cone

The regenerating blastema cone formed 14–16 days post-amputation appears like a dark cone with a soft consistence (lower inset in Figure 1a). The histological examination of the blastema reveals a loose connective tissue mainly comprising mesenchymal cells (irregular-shaped) and fibroblasts (with a bipolar shape) located underneath a multilayered wound (regenerating) epidermis (Figure 1a and upper inset). The observation under transmission electron microscopy shows roundish or elongated mesenchymal cells that are separated one from another from broad spaces containing little and flocculent extracellular material and sparse non-banded collagen fibrils (Figure 1b,c). The cytoplasm of blastema cells contains mainly ribosome, linear or rosette-like polysomes while the endoplasmic cisternae are generally scarce in these cells (Figure 1d,e). The nucleolus is developed in most blastema cells and evidences various combinations of denser fibrillar areas and sparse granular region while pale fibrillar centres are scarce or absent (Figures 1f and 2a). The granular component appears prevalent on the fibrillar component, and a granular cortex is often seen in central or more tangential sections of the nucleolus. An apical ependymal ampulla is present in the central position of the blastema, as the continuation of the spinal cord of the tail stump. The ependyma is composed of few epithelial cells in comparison with the majority of mesenchymal cells and fibroblasts forming the blastema (Figures 1a and 2b).

The active proliferation of the blastema was revealed by 5BrdU immunolabelling at the light and electron microscope. After 4 h from 5BrdU injection, the nuclear 5BrdU immunolabelling indicates that sparse proliferating cells are commonly detected in the mesenchyme of the blastema (Figure 2c,d). Also the thick wound epithelium of the blastema (Figure 3a,b) shows sparse labelled cells among unlabelled keratinocytes (Figures 2c and 3c). The study at higher magnification of wound keratinocytes mainly shows that they contain free ribosomes, linear or rosette-organized polysomes among sparse bundles of keratin. Ribosomes decrease in the cytoplasm of keratinocytes present in the upper layers where they are differentiating (Figure 3d). The nucleolus of basal and suprabasal keratinocytes (spinosus layers) also shows prevalence of the granular component over the dense fibrillar component (Figure 3e). In precorneous layers of the wound epidermis, transitional keratinocytes contain less ribosomes while electron-pale lipid droplets and dense roundish granules of 0.2–0.5 μm in diameter become abundant. Lipids occupy the central area of maturing corneocytes while keratin bundles and dense granules remain marginal (Figure 3f). Lipids disappear in the thin and fully mature corneocytes of the wound epidermis. These morphological observations indicate that blastema (mesenchymal) cells and undifferentiated keratinocytes of the thick wound epidermis are the more abundant cell types that provide the RNA for extraction in the present analysis.

3.2 | ncRNA variations between regenerating and normal tail

Four snoRNA genes here studies (*scarna11*, *snord63*, *snord74* and *snord26*) are exclusively expressed in the regenerating tail blastema while other three are also detected in the limb (*snord87*, *U2*, *U4*; Alibardi, 2019a; Vitulo et al., 2017a). The ncRNAs genes here analysed appear upregulated in the regenerating tail, with the exception of *snord87*, indicating that they are involved in the developmental process (Figures 4 and 5). The relative expressions indicated from the folds of ncRNAs variations in non-normalized trials appear higher for *snord26*, *snord74* and *snord63* than for *scarna11* (Figure 4a). Instead, *snord87*, is slightly lower expressed in the regenerating than in normal tail. Much higher values, stressing the difference between normal and regenerating tails are obtained for U2 and U4 snRNAs (Figure 4b). When the expression folds are instead referred to *gapdh* expression level for each ncRNA (normalized), they show the highest variation for *scarna 11*, *U2* and *U4* (Figure 5). The intervals shown on top of each column in Figures 4 and 5 indicate that the noted differences between normal versus regenerating tail are all statistically significant. As a side note, although utilized a referring enzyme *gapdh* (glyceraldehyde-3-phosphate dehydrogenase) expression appears itself quite

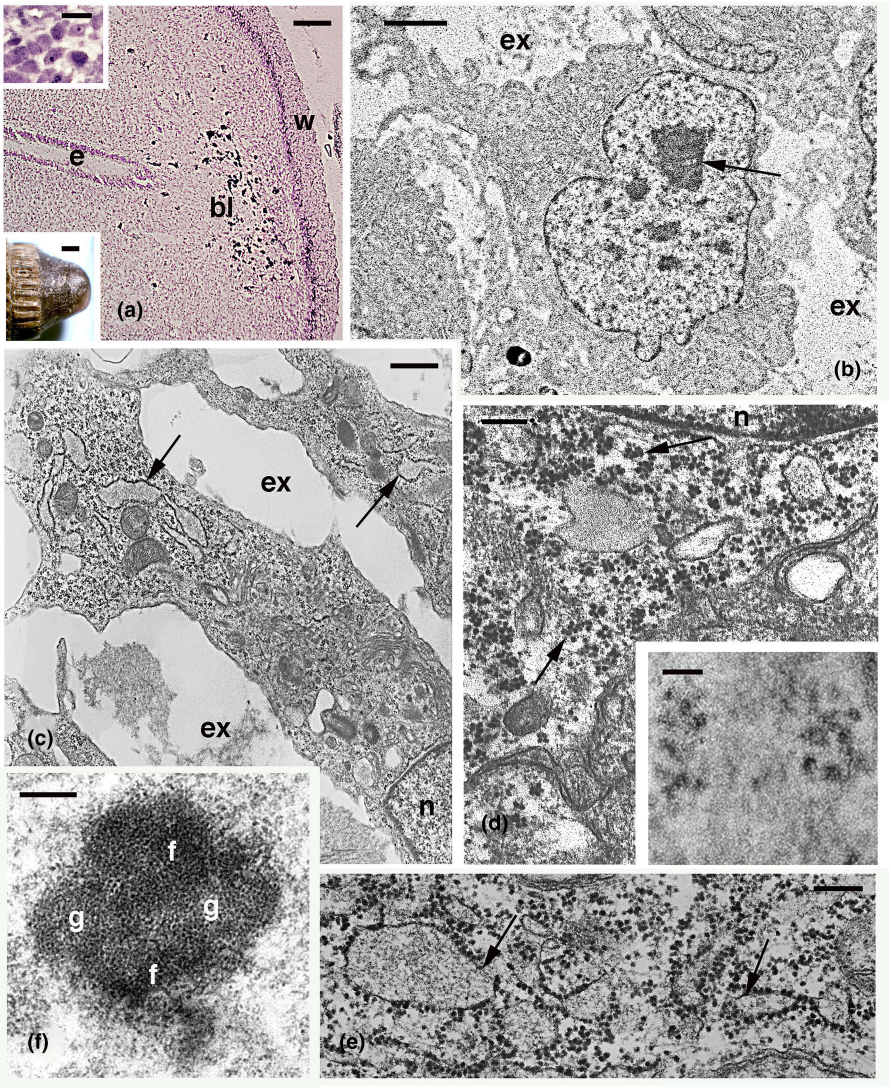

FIGURE 1 Light (a) and transmission electron microscope views (b–f) of mesenchymal cells in the blastema. (a) general aspect of the blastema. Toluidine blue stain. Bar, 50 μm. Lower inset (Bar, 0.5 mm) shows a blastema. Upper inset (Bar, 10 μm) shows blastema cells. (b) blastema cell featuring a large nucleolus (arrow). Bar, 1 μm. (c) elongated cells containing sparse endoplasmic cisternae (arrows). Bar, 0.5 μm. (d) close-up to the cytoplasm of a cell occupied by most clusters of rosette polyribosomes (arrows). Bar, 200 nm. The inset (Bar, 100 nm) shows polysomes. (e) cytoplasm featuring free ribosomes and some associated to endoplasmic cisternae (arrows). Bar, 200 nm. (f) nucleolus with dense fibrillar component among most granular component. Bar, 250 nm. bl, blastema; e, ependymal; ex, extracellular space/matrix; f, fibrillar (dense) component; g, granular component; n, nucleus; w, wound (regenerating) epidermis.

high in the regenerating blastema (see interpretation of this datum in Discussion).

4 | DISCUSSION

4.1 | General consideration on snoRNAs and snRNAs on protein synthesis

Previous studies on variations of the total RNAs content and its distribution in regenerating tails of *P. muralis*, *P. sicula* and other lizards indicated that the stages of blastema and early cone (Figure 6a–d) are those synthetically more active for RNA and protein synthesis and for cell multiplication (Alibardi, 2014; Alibardi & Sala, 1983, 1988; Cox, 1969; Gilbert et al., 2015; Shah et al., 1977). In elongating cones, an intense cell proliferation and RNA distribution is only observed in the distal regions of the early muscle aggregates, in the apical ependymal tube and in the initial cartilaginous tissues that gives rise to the new axis of the regenerating tail (Figure 6e). Cell proliferation rapidly lowers and disappears in differentiating tissues of the elongating tail.

Using RQ-PCR, the present study has shown a significant increase of snoRNAs in the growing blastema in comparison with the normal tail, confirming a previous transcriptome study (Vitulo et al., 2017a, 2017b). The exclusive presence of four snoRNAs (*snora63*, *snord74*, *scarna11* and *snord26*) only in the tail blastema, but not in the healing limb, suggested that these ncRNAs have an important role in the process of regeneration (Alibardi, 2019a, 2021; Vitulo et al., 2017a). The other ncRNAs, *snord87*, *U2* e *U4* are instead up-regulated also in the amputated limb. The increase of expression of snoRNAs has also evidenced a high expression of *gapdh* in regenerated blastemas, a glycolytic enzyme converting 3-phospho-glyceraldehyde into 1,3-diphospho-glycerate. Although *gapdh* expression is usually constant in most cells it appears variably expressed in regenerating versus normal tissues (Figure 4). Therefore, the normalization of

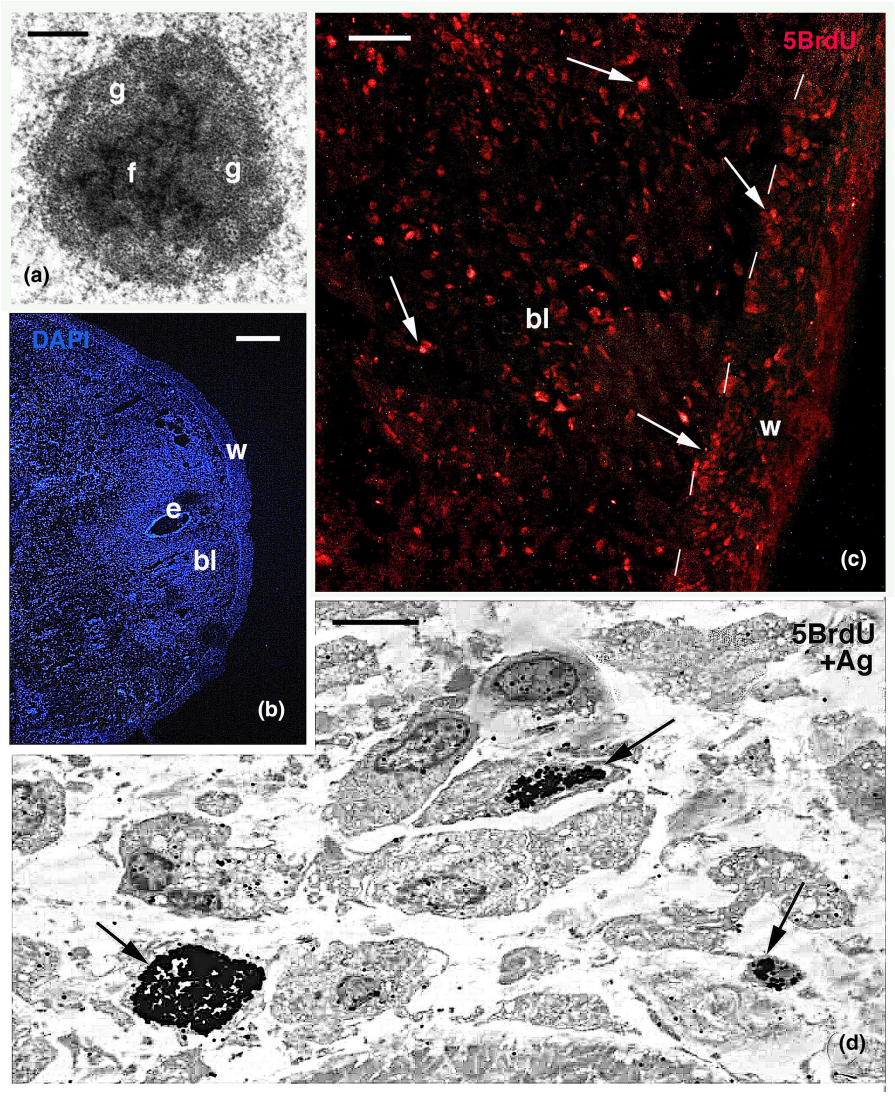

FIGURE 2 Electron microscopic (a, d) and fluorescent (b, c) images of regenerative blastema. (a) detail of large nucleolus. Bar, 250 nm. (b) DAPI fluorescence showing the cell density in the blastema. Bar, 50 μm. (c) detail of 5BrdU labelling evidencing sparse-labelled cells (arrows). Bar, 20 μm. (d) immunogold with silver enhancement of 5BrdU-labelled cells (nuclei, arrows) in the blastema. Bar, 5 μm. bl, blastema; e, ependymal; f, fibrillar component; g, granular component; w, wound epidermis.

expression (Figure 5) has allowed to confirm that there is a significant overexpression of most ncRNAs in the regenerating blastema. This result supports previous studies indicating that the regenerative blastema, like for cancer cells, undergo a Warburg effect as it mainly utilizes a glycolytic metabolism and the pentose phosphate shunt for producing energy and ribonucleotides (Alibardi, 2014; Shah et al., 1977). Gapdh has also other physiological roles in the cell including activation of transcription (Zhang et al., 2015), further confirming that blastema cells rapidly synthetize high levels of proteins.

In general, snoRNAs intervene in the 2-ortho-methylation (2′-*O*-methylation, C/D snord) and pseudourydination (H/ACA snora) of rRNAs, and this process influence the activities of ribosomes on the translation process, both in terms of speed, precision and timing of translation (Dupuis-Sandoval et al., 2015; Makarova et al., 2013; McMahon et al., 2015), the latter particular important for cell multiplication and growth. Another function of snoRNAs is related to chromatin de-condensation, maintaining open some regions of the chromosomes for transcription (chromatin remodelling) and therefore controlling also this process. Many snoRNAs are also precursors of some miRNAs, molecules that intervene in the process of cell differentiation, and specific miRNAs have been also detected in the regenerating tail of lizard (Hutchins et al., 2016). Finally *U2*, *U4* snRNAs and some snoRNAs modulate the process of splicing and ribosomal translation by altering pre-mRNAs (Morais et al., 2021). Numerous genes for snoRNAs are localized within introns of some coding genes, and they are transcribed from RNApolymerase II. Other snoRNAs are instead derived from inter-genic regions. The importance of non-coding genes on organ regeneration has also been suggested observing their derivation from the long intronic sequences present in the large genomes of "regenerative-competent" amphibians and fish (Nogueira et al., 2016; Nowoshilov et al., 2018; Smith et al., 2009).

The granular cortex observed in the nucleolus of blastema cells and in wound keratinocytes (Figures 1f, 2a

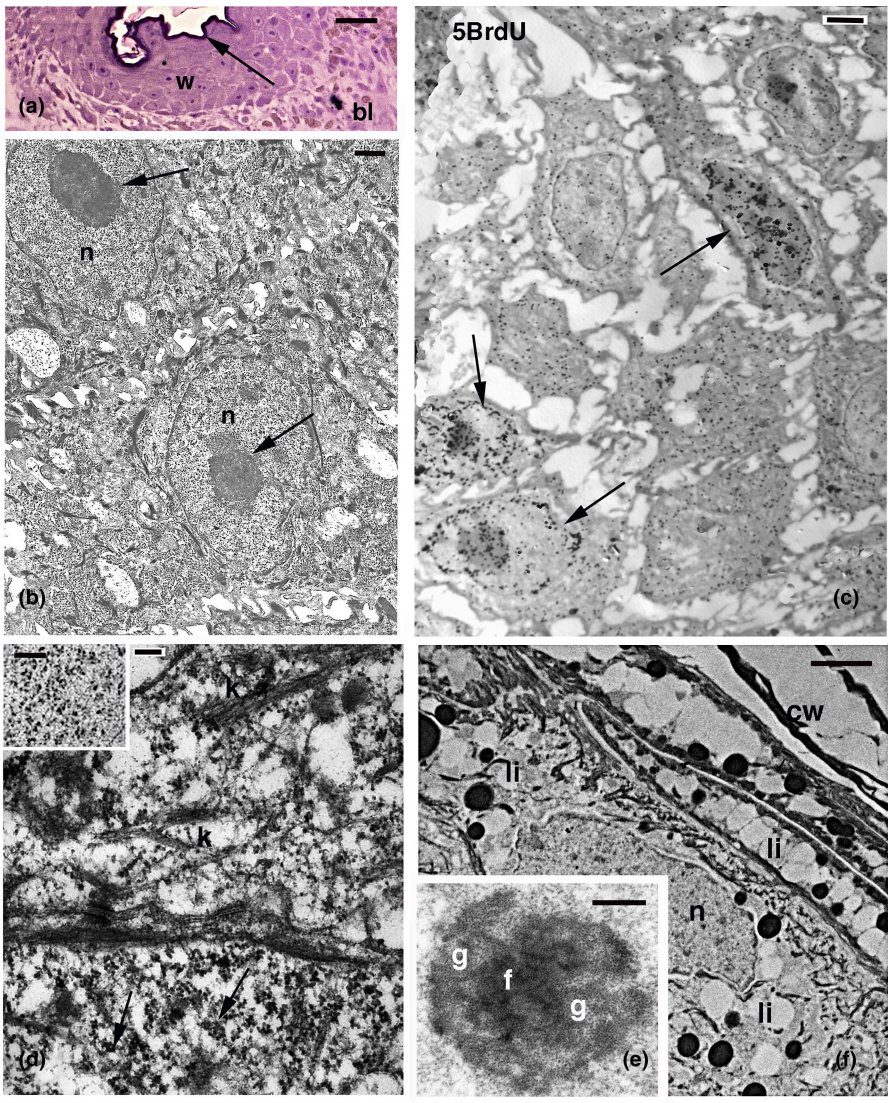

FIGURE 3 Light (a) and electron microscopy (b–e) view wound keratinocytes. (a) stratified epidermis of the blastema with thin (initial) stratum corneum (arrow). Toluidine blue stain. Bar, 10 μm. (b) detail on spinosus keratinocytes with large nucleoli (arrows). Bar, 0.5 μm. (c) 5BrdU-labelled wound keratinocytes (nuclei, arrows). Immunogold with silver intensification. Bar, 1 μm. (d) detail of the cytoplasm of suprabasal keratinocyte with rosette-shaped polysomes (arrows). The upper, differentiating cell contains bundles of keratin and a lower number of ribosomes. Bar, 200 nm. The inset (Bar, 200 nm) shows free ribosomes. (e) close-up to a nucleolus. Bar, 250 nm. (f) differentiating keratinocyte localized beneath the flattening cells of the forming corneous layer. Bar, 0.5 μm. bl, blastema; cw, corneocytes of the wound epidermis; f, fibrillar component; g, granular component; k, keratin bundle; li, lipids; n, nucleus.

and 3e) indicates an intense exchange of pro-ribosomes directed towards the cytoplasm of blastema cells for protein synthesis (Lamaye et al., 2011). Although a direct proof is lacking, we suggest that some ribosome selection and intense splicing processes take place in blastema cells, and that ribosomes not only increase in number but also become more efficient in protein synthesis. The variation in the quality of ribosomes has been also hypothesized for cancer cells where they form ribosomes very active in protein synthesis for sustaining a continuous cell multiplication (Penzo et al., 2019; Xue & Barna, 2012).

4.2 | Hypothetic roles for the ncRNAs detected in *P. muralis* blastema

It is known that during development, aside coding genes, also numerous non-coding genes are activated and participate in essential processes for the morphogenesis of numerous organs. The stage of regeneration here utilized (Figures 1 and 6a–c) mainly includes cells of mesenchymal and fibroblast type in addition to wound (regenerating) keratinocytes among which numerous keratinocytes are proliferating (Alibardi, 2014, 2016, 2019b). Therefore, the RNAs, including ncRNAs extracted in the present study and during transcriptome analysis (Vitulo et al., 2017a), most likely derive from the prevalent mesenchymal and epidermal cells of the blastema while a minor contribution in RNAs is obtained from the less represented cells present at this early stage in the growing blastema (blood, nerves, ependyma, myoblasts and chondroblasts).

In the apical regions of the regenerating cone, cell proliferation is continuous, likely stimulated from coding and snoRNAs oncogenes (Alibardi, 2019a, 2022; Degan et al., 2020). This activity changes as the blastema becomes conical and the more proximal cells, close to the tissues of the tail stump, begin differentiation (Figure 6d). General information on the roles of ncRNAs is reported in the Catalogue Rfam/Wikipedia book at http://code.pediapress.com/ 2010 and from

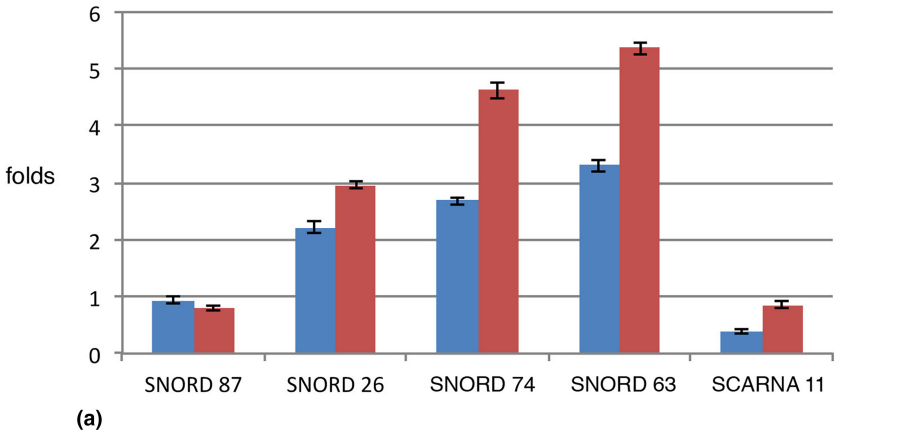

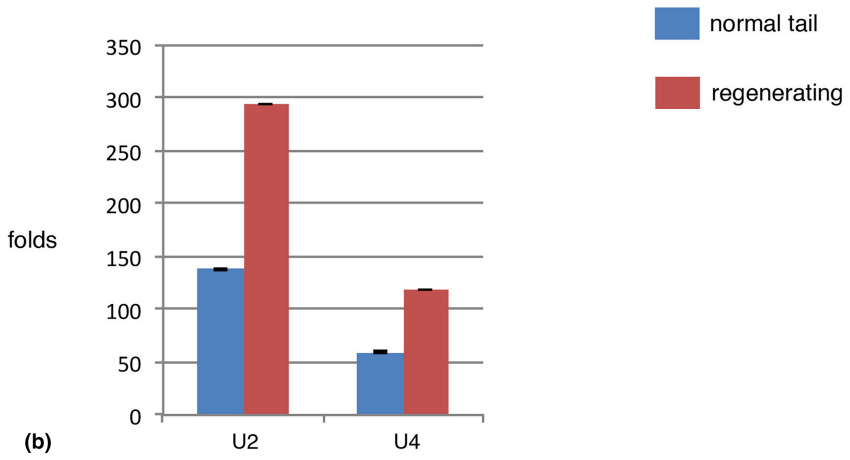

FIGURE 4 Non-normalized relative expression ($\Delta\Delta C_t$ on the weighted average between trials) for different ncRNAs detected in our experiments on normal versus regenerating tail tissues. In A are shown ncRNAs variations of a lower scale while in B are reported much higher values of variation (for U2 and U4 snRNAs).

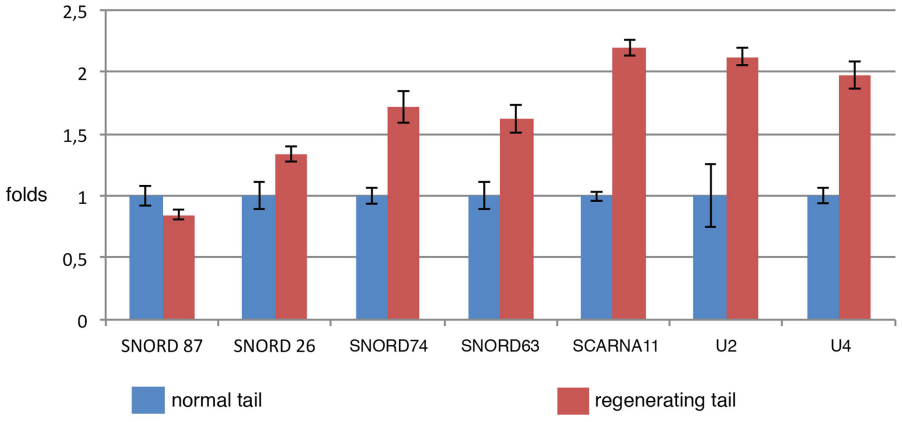

FIGURE 5 Normalized expression ($2^{-\Delta\Delta C_t}$ on the weighted average between trials, referred to *gapdh*) for different ncRNAs in normal versus regenerated tail tissues. This histogram confirms the overexpression of these ncRNAs detected in the previous relative expression histogram.

previous studies (Dupuis-Sandoval et al., 2015; Makarova et al., 2013; McMahon et al., 2015). Three out of the four snoRNAs here analysed (*snord87*, *snord74*, *scarna 11*) guide modifications in the rRNA 28S while *snora63* guide changes in the rRNA 18S. These snoRNAs also influence the activity of *U2* and *U4* in the process of splicing. Snora63 (H/ACA class) participates in the pseudourydilation of rRNA 18S and in the regulation of ribosome translation of the initiator factor 4II. *Snord74* (H/ACA class) determines increase in activity of rRNAs still located in the nucleolus and is associated with pathologies such as leukaemia and multiple myeloma (McMahon et al., 2015). *Scarna11* operates the pseudourydilation within the splicing particle including *U2* and *U4* snRNAs derived from RNApolymerase II transcription, a process that accelerates transcription and migration of mRNAs in the cytoplasm for protein synthesis (Morais et al., 2021). *Scarna11* also activates the maturation and activity of the template RNA strand (TR) of the telomerase enzyme (TERT), an enzyme that has been detected in the early blastema of lizards (Alibardi, 2019a).

In general these snoRNAs and snRNAs appear as most likely oncogenes stimulating the proliferation of blastema cells while the function of the two ncRNAs with

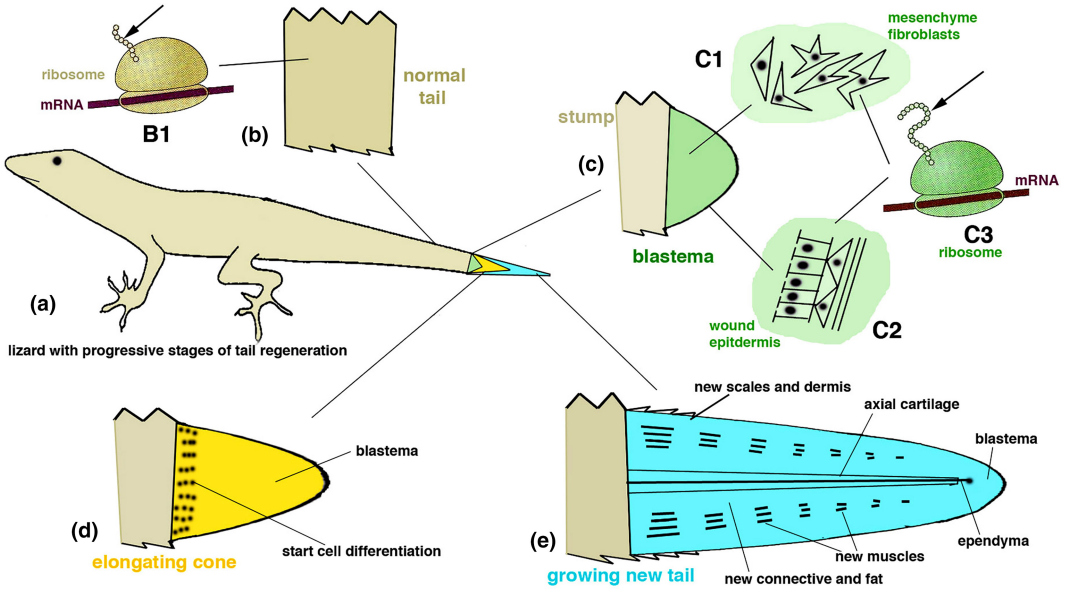

FIGURE 6 Schematic drawing presenting the hypothesis that based on the up-regulation of ncRNAs some ribosomes in the regenerating blastema cells (c-c3) can synthesize proteins at a faster rate that ribosomes of fully differentiated tissues and mature fibrocytes of the normal tail (a-b1). The arrows in b1 and c3 indicate the longer peptides produced in blastema cells (mesenchyme and wound epidermis) at the same time as the shorter peptide of normal tail cells. As a result of the higher protein synthesis, the blastema elongates into a cone where only the more proximal regions start cell differentiation (d) and rapidly into a growing new tail where numerous tissues are differentiated and growing (e).

the lower expression (relative and absolute), *snord26* and *snord87*, is less defined. In case they may also act as tumour suppressors their hypothesized inhibitory action is however overcome by the expression of the other ncRNAs (Figures 4 and 5) and also from codingRNAs such as *wnts*, *egfr* and *fgfr* at the early blastema stage (Degan et al., 2020). The prevalence of oncogenes expression determines a net growth of the initial blastema cone, but the process decreases at later stages when tumour suppressors likely determine tissue differentiation. *Snord26* (H/ACA class) operates the pseudourydilation of rRNA 28S and is present in snRNPs where it enhances the activity of rRNA. In other organs, the increase of *Snord26* activity is associated with colon carcinoma, but it also appears as an inhibitor (tumour suppressor) in other types of cancer (Parson et al., 2018). *Snord87* (C/D class) induce 2′-*O*-methylation of snRNAs in the nucleolus, including rRNA 18S, but its role as oncogene or tumour suppressor remains unknown. It therefore appears that oncogenes favour cell proliferation needed for the formation and initial growth of the blastema cone.

Finally the two snRNA, *U2* and *U4*, appear correlated to the splicing process (Morais et al., 2021) that occurs in blastema cells, likely accelerating it for a massive production of mRNAs. *U2* is a snRNA of the spliceosome complex that is involved in the splicing of pre-mRNAs while *U4* is a snRNA component of the *U2* snRNA of spliceosomes and may have an inhibitory action on spliceosome catalytic activity (tumour suppressor?). Although the above discussion indicates a general increase in activity of ribosome and splicing in blastema cells influenced by these snoRNAs, further studies are needed for discovering the specific functions of these ncRNAs during tail regeneration and how their action is contrasted by some tumour suppressors in order to regulate tail regeneration.

In conclusion, given the known localization of ncRNAs in different cells of vertebrates previous and the present results indicate that mesenchymal cells and keratinocytes of the early regenerating tail in *P. muralis* overexpress 6 ncRNAs (*snord26*, *snord74*, *snora63*, *scarna11*, *U2* and *U4*), likely involved in enhancing ribosome activity and pre-mRNA splicing. Only *snord87*, remains unchanged or is down-regulated in comparison with the normal tissues. The study hypothesizes that these snoRNAs stimulate the formation of more efficient ribosomes in blastema cells that increase protein synthesis and allow the rapid growth of the blastema into a new tail (Figure 6).

ACKNOWLEDGEMENTS

The study was supported by Centro di Riferimento Oncologico, Aviano, PN (Massimo Degan) and by Comparative Histolab Padova (Lorenzo Alibardi).

CONFLICT OF INTEREST STATEMENT

The authors declare no conflicts of interest.

ORCID

Lorenzo Alibardi https://orcid.org/0000-0002-8247-2217

REFERENCES

Alibardi, L. (2010). Ultrastructural features of the process of wound healing after tail and limb amputation in lizard. *Acta Zoologica*, *91*, 306–318.

Alibardi, L. (2014). Histochemical, biochemical and cell biological aspects of tail regeneration in lizard, an amniote model for studies on tissue regeneration. *Progress in Histochemistry and Cytochemistry*, *48*, 143–244.

Alibardi, L. (2015). Regeneration of the articular cartilage in lizard knee from resident stem cells. *International Journal of Molecular Sciences*, *16*, 20731–20747.

Alibardi, L. (2016). Cell proliferation in the amputated limb of lizard leading to scarring is reduced compared to the regenerating tail. *Acta Zoologica*, *98*, 170–180.

Alibardi, L. (2017). Immunolocalization of sonic hedgehog and patched in the regenerating tail of lizard suggests they are involved in cell proliferation and epidermal differentiation. *BAOJ Dermatology*, *1*, 004.

Alibardi, L. (2019a). Review: The regenerating tail blastema of lizard as a model to study organ regeneration and tumor growth regulation in amniotes. *Anatomical Record*, *302*, 1469–1490.

Alibardi, L. (2019b). Temporal distribution of 5BrdU-labeled cells suggests that most injured tissues contribute proliferating cells for the regeneration of the tail and limb in lizard. *Acta Zoologica*, *100*, 303–319.

Alibardi, L. (2021). Review. Tail regeneration in Lepidosauria as an exception to the generalized lack of organ regeneration in amniotes. *Journal of Experimental Zoology*, *336B*, 145–164.

Alibardi, L. (2022). Letter to the editor. Organ regeneration occurs in vertebrate with aquatic-related life cycles including metamorphosis and was lost during land transition. *Integrative and Comparative Biology*, *62*, 121–123.

Alibardi, L., & Sala, M. (1983). Distribuzione di sostanze d'importanza morfogenetica in tessuti rigeneranti di *Lacerta sicula*, *Triturus alpestris* e *Rana dalmatina*. *Atti e Memorie Accademia Patavina Scienze, Lettere e Arti*, *95*, 100–151.

Alibardi, L., & Sala, M. (1988). Fine structure of the blastema in the regenerating tail of the lizard *Podarcis sicula*. *Bollettino di Zoologia*, *55*, 307–313.

Bellairs, A. A., & Bryant, S. V. (1968). Effects of amputation on limbs and digits of lacertid lizards. *Anatomical Record*, *161*, 489–495.

Bomben, R., Dal-Bo, M., Benedetti, D., Capello, D., Forconi, F., Marconi, D., Bertoni, F., Maffei, R., Laurenti, L., Rossi, D., Del Principe, M. I., Luciano, F., Sozzi, E., Cattarossi, I., Zucchetto, A., Rossi, F. M., Bulian, P., Zucca, E., Nicoloso, M. S., … Gattei, V. (2010). Expression of mutated *IGHV3-23* genes in chronic lymphocytic leukemia identifies a disease subset with peculiar clinical and biological features. *Clinical Cancer Research*, *16*, 620–628.

Cox, P. G. (1969). Some aspects of tail regeneration in the lizard *Anolis carolinensis*. II. The role of the peripheral nerves. *Journal of Experimental Zoology*, *171*, 151–160.

Degan, M., Dalla Valle, L., & Alibardi, L. (2020). Gene expression in regenerating and scarring tails of lizard evidences three main key genes (*wnt2b*, *egfl6* and *arhgap28*) activated during the regulated process of tail regeneration. *Protoplasma*, *258*, 3–17.

Dupuis-Sandoval, F., Poirier, M., & Scott, M. S. (2015). The emerging landscape of small nucleolar RNAs in cell biology. *Wiley Interdisciplinary Review RNA*, *6*, 381–397.

Fisher, R. E., Geiger, L. A., Stroik, L. K., Hutchins, E. D., George, R. M., DeNardo, D. F., Kusumi, K., Rawls, J. A., & Wilson-Rawls, J. (2012). A histological comparison of the original and regenerated tail in the green anole, *Anolis carolinensis*. *Anatomical Record*, *295*, 1609–1619.

Gilbert, E. A., Delorme, S. L., & Vickaryous, M. K. (2015). The regeneration blastema of lizards: An amniote model for the study on appendage replacement. *Regeneration*, *2*, 45–53.

Grygorian, E. N. (2021). Study of natural longlife juvenility and tissue regeneration in caudate amphibians and potential application of resulting data in biomedicine. *Journal of Developmental Biology*, *9*, 2.

Hutchins, E. D., Eckalbar, W. L., Walter, J. M., Mangone, M., & Kosumi, K. (2016). Differential expression of conserved and novel microRNAs during tail regeneration in the lizard *Anolis carolinensis*. *BMC Genomics*, *17*, 339.

Hutchins, E. D., Markov, G. J., Eckalbar, W. L., Gorge, R. M., King, J. M., Tokuyama, M. A., Geiger, L. A., Emmert, N., Ammar, M. J., Allen, A. P., Siniard, A. L., Corneveaux, J. J., Fisher, R. E., Wade, J., DeNardo, D. F., Rawls, J. A., Huentelman, M. J., Wilson-Rawls, J., & Kusumi, K. (2014). Transcriptomic analysis of tail regeneration in the lizard *Anolis carolinensis* reveals activation of conserved vertebrate developmental and repair mechanisms. *PLoS One*, *9*, e105004.

Lamaye, F., Galliot, S., Alibardi, L., Lafontaine, D. L., & Thiry, M. (2011). Nucleolar structure across evolution: The transition between bi- and tri-compartimentalized nucleoli lies within the class Reptilia. *Journal of Structural Biology*, *174*, 352–359.

Lozito, T. P., & Tuan, R. S. (2016). Lizard tail skeletal regeneration combines aspects of fracture healing and blastema-based regeneration. *Development*, *143*, 2946–2957.

Makarova, J. A., Ivanova, S. M., Tonevitsky, A. G., & Grigoriev, A. I. (2013). New functions of small nulceolar RNAs. *Biochemistry (Moscow)*, *78*, 638–650.

McMahon, M., Contreras, A., & Ruggero, D. (2015). Small RNAs with big implications: New insights into H/ACA snoRNA function and their role in human disease. *Wiley Interdisciplinary Review RNA*, *6*, 173–189.

Mescher, A. L. (2017). Macrophages and fibroblasts during inflammation and tissue repair in models of organ regeneration. *Regeneration*, *4*, 39–53.

Morais, P., Adachi, H., & Yu, Y. T. (2021). Spliceosomal snRNA epitranscriptomics. *Frontiers in Genetics*, *12*, 652129.

Nogueira, A. F., Costa, C. M., Lorena, J., Moreira, R. N., Frota-Lima, G. N., Furtado, C., Robinson, M., Amemiya, C. T., Darnet, S., & Schneider, I. (2016). Tetrapod limb and sarcopterygian fin regeneration share a core genetic program. *Nature Communications*, *7*, 13364. https://doi.org/10.1038/ncomms13364

Nowoshilov, S., Schloissnig, S., Feng-Fei, J., Pang, A. D., Pippel, M., Winkler, S., Hastie, A. R., Young, G., Roscito, J. G., Falcon, F., Knapp, D., Powell, S., Cruz, A., Cao, H., Habermann, B., Hiller, M., Tanaka, E. M., & Myers, E. W. (2018). The axolotl genome

and the evolution of key tissue formation regulators. *Nature*, *554*, 50–56.

Parson, C., Tayoun, A. M., Benado, B. D., Ragusa, G., Dorvil, R. F., Rourke, E. A., O'Conner, K., Reed, I. G., Alexander, A., Willetts, L., Habibian, M., & Adams, B. D. (2018). The role of long non-coding RNAs in cancer metastasis. *Journal of Cancer and Metastasis Treatments*, *4*, 19.

Patel, S., Ranadive, I., Buch, P., Khaire, K., & Balakrishnan, S. (2022). De novo transcriptome sequencing and analysis of differential gene expression among various stages of tail regeneration in *Hemidactylus flaviviridis*. *Journal of Developmental Biology*, *10*, 24.

Penzo, M., Montanaro, L., Treré, D., & Derenzini, M. (2019). The ribosome biogenesis—Cancer connection. *Cell*, *8*, 55.

Pritchard, J. J., & Ruzicka, A. J. (1951). Comparison of fracture repair in the frog, lizard and rat. *Journal of Anatomy*, *84*, 236–262.

Reichman, O. J. (1984). Evolution of regeneration capabilities. *American Naturalist*, *123*, 753–763.

Scala, C., Cenacchi, G., Ferrari, C., Pasquinelli, G., Preda, P., & Manara, G. C. (1992). A new acrylic resin formulation: A useful tool for histological, ultrastructural, and immunocytochemical investigations. *Journal of Histochemistry and Cytochemistry*, *40*, 1799–1804.

Shah, R. V., Kothari, J. S., & Hiradhar, P. K. (1977). Alterations in certain metabolites during tail regeneration in the gekkonid lizard, *Hemidactylus flaviviridis*. *Journal of Animal Morphology and Physiology*, *24*, 65–75.

Smith, J. J., Putta, S., Zhu, W., Pao, G. M., Verma, I. M., Hunter, T., Bryant, S. V., Gardiner, D. M., Harkins, T. T., & Voss, S. R. (2009). Genic regions of a large salamander genome contain long introns and novel genes. *BMC Genomics*, *10*, 19.

Vitulo, N., Dalla Valle, L., Skobo, T., Valle, G., & Alibardi, L. (2017a). Transcriptome analysis of the regenerating tail versus the scarring limb in lizard reveals pathways leading to successful versus unsuccessful organ regeneration in amniotes. *Developmental Dynamics*, *246*, 116–134.

Vitulo, N., Dalla Valle, L., Skobo, T., Valle, G., & Alibardi, L. (2017b). Down-regulation of lizard immuno-genes in the regenerating tail and myo-genes in the scarring limb suggests that tail regeneration occurs in an immuno-privileged organ. *Protoplasma*, *254*, 2127–2141.

Xue, S., & Barna, M. (2012). Specialized ribosomes: A new frontier in gene regulation and organismal biology. *Nature Reviews Molecular Cell Biology*, *13*, 355–369.

Zhang, J. Y., Zhang, F., Hong, C. Q., Giuliano, A. E., Cui, X. J., Zhou, G.-J., Zhang, G. J., & Cui, Y. K. (2015). Critical protein GAPDH and its regulatory mechanisms in cancer cells. *Cancer Biology & Medicine*, *12*, 10–22.

SUPPORTING INFORMATION

Additional supporting information can be found online in the Supporting Information section at the end of this article.

How to cite this article: Degan, M., & Alibardi, L. (2023). SnoRNAs may accelerate protein synthesis for the rapid growth of the regenerating tail blastema in the lizard *Podarcis muralis*. *Acta Zoologica*, *00*, 1–11. https://doi.org/10.1111/azo.12477